

## Out-of-equilibrium stationary states, percolation, and subcritical instabilities in a fully nonconservative system

Mathieu Génois,<sup>1,2,\*</sup> Pascal Hersen,<sup>1</sup> Eric Bertin,<sup>3</sup> Sylvain Courrech du Pont,<sup>1</sup> and Guillaume Grégoire<sup>1,4,†</sup>

<sup>1</sup>*Laboratoire Matière et Systèmes Complexes (MSC), Université Paris-Diderot, CNRS UMR 7057, F-75205 Paris Cedex 13, France*

<sup>2</sup>*CPT, Aix-Marseille Université, Université de Toulon, CNRS, UMR 7332, F-13288, Marseille, France*

<sup>3</sup>*LIPHY, Université Grenoble Alpes and CNRS, F-38000 Grenoble, France*

<sup>4</sup>*HPC Institute (ICI), École Centrale, Nantes, 1 rue de la Noë, F-44300 Nantes, France*

(Received 18 March 2016; published 3 October 2016)

The exploration of the phase diagram of a minimal model for barchan fields leads to the description of three distinct phases for the system: stationary, percolable, and unstable. In the stationary phase the system always reaches an out-of-equilibrium, fluctuating, stationary state, independent of its initial conditions. This state has a large and continuous range of dynamics, from dilute—where dunes do not interact—to dense, where the system exhibits both spatial structuring and collective behavior leading to the selection of a particular size for the dunes. In the percolable phase, the system presents a percolation threshold when the initial density increases. This percolation is unusual, as it happens on a continuous space for moving, interacting, finite lifetime dunes. For extreme parameters, the system exhibits a subcritical instability, where some of the dunes in the field grow without bound. We discuss the nature of the asymptotic states and their relations to well-known models of statistical physics.

DOI: [10.1103/PhysRevE.94.042101](https://doi.org/10.1103/PhysRevE.94.042101)

### I. INTRODUCTION

One of the key assumptions of equilibrium statistical physics is the existence of conservation laws associated to quantities like energy, linear and angular momenta, and number of particles. Out of equilibrium, some of the conservation laws may break. In driven systems, some of the mechanical quantities are continuously injected and dissipated into the surrounding medium [1]. In reaction-diffusion problems [2,3], even the conservation of the number of particles may be absent. Systems without conservation laws often exhibit an absorbing phase transition (APT) between an active phase with a fluctuating number of particles, and an absorbing phase without any activity. Depending on the model, it could be a state where all particles have disappeared, or where particles are in a frozen state. A prominent universality class for absorbing phase transitions is the directed percolation (DP) class [4,5]. But the definition of a class of universality is very sensitive to the underlying symmetries: parity of the number of reactants [6], nature of the absorbing phase [7], etc., imply different universality classes from DP. Furthermore, if a source of noise has an effect on the absorbing phase, it seems that the phase transition disappears [4,8].

In reaction-diffusion models, the dynamics is defined in terms of particles, and the order parameter is linked to the number of particles. In other models, the dynamics acts on a continuous additive quantity: mass, energy, or momentum. Related phase transitions happen between a low, even fluctuating, homogeneous level of this quantity and a localized state where it is maximized. For instance, in systems of self-propelled particles [9], the momentum is zero on average in the disordered phase, whereas it is concentrated in solitons, or in nonlinear, periodic peaks [10,11] in the “ordered” phase. In mass transfer models (MTMs) [12], an out-of-equilibrium

activity maintains the exchange of mass between sites and leads to a transition of mass condensation on few sites.

Previously [13,14], geophysical matters have led us to build a model for barchan fields in order to understand the peculiar characteristics of such structures. Our studies were based on experiments [15,16] and on field observations [17–19]. However, we will now ignore the natural background of the model to study its whole phase diagram. We consider objects, which we will arbitrarily call *dunes* and which are characterized by an extensive quantity  $V$  that we will call *volume*, but could as likely be either mass or energy. Those objects appear, move spatially, react with each other, and disappear depending on the value of  $V$ .

This model presents features similar to both reaction-diffusion models and MTMs. One can wonder whether a symmetry will govern the properties of the system and its phase transition, or if we get a richer phase diagram. We propose now to investigate the parameter space of our system to understand the interplay between both ingredients.

In the following, we define our model. We question its microscopic symmetries and we present the (classical) models of statistical physics to which we expect to compare our dunes model. Then, with numerical measurements and analytical arguments, we will show that percolated noisy deserts can be found. Finally, in an opposite limit of the control parameters, we find a transition of dune condensation.

### II. DESCRIPTION OF THE MODEL

In this model, cubic dunes are labeled by their position  $(x, y)$  on the field and their size  $w = V^{1/3}$ . These variables are continuous, as neither the space nor the size are discretized. Dunes move on the field in the decreasing  $y$  direction only [Fig. 1(a)], with a speed  $v$  inversely proportional to their size:

$$v = \frac{\alpha}{w}, \quad (1)$$

\*Mathieu.Genois@cpt.univ-mrs.fr

†guillaume.gregoire@ec-nantes.fr

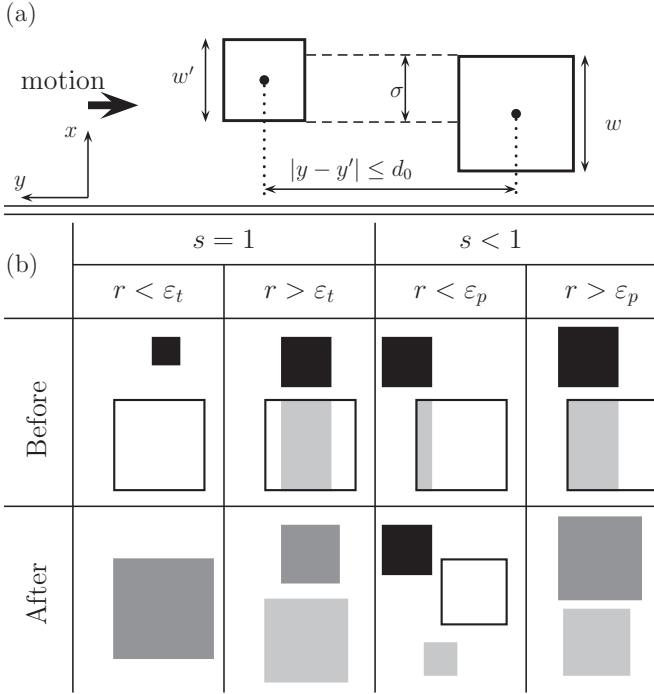


FIG. 1. Interactions between dunes. (a) Remote interaction and definition of the neighborhood. (b) The four types of ideal collisions: merging, exchange with  $s = 1$ , fragmentation, exchange with  $s < 1$ .

where  $\alpha$  is a parameter which is related to the mobility of a dune.

The field has a length  $L$  and a width  $\ell$ . We impose biperiodic conditions at the borders of the field, ensuring that dunes reaching the  $y = 0$  limit (respectively  $x = 0$ ) are going on their ways at the  $y = L$  border (respectively  $x = \ell$ ), and vice versa.

The size of a single dune decreases in time according to the following law:

$$w(t) = [w^3(t_0) - (t - t_0)\Phi]^{1/3}, \quad (2)$$

where  $w(t_0)$  is the initial size of the dune,  $t_0$  is the time it appears on the field, and  $\Phi$  is the constant rate of volume loss. This law is valid until the size of the dune reaches the minimum value  $w_m$ , when it is then removed from the field. To compensate for this outflux, dunes of size  $w_0$  are injected on the field, randomly in time and space, at a constant mean rate  $\lambda$  by units of time and surface.

Dunes interact with each other in two different ways. If two dunes are closer than a distance  $d_0$  along the  $y$  direction and the overlap length  $\sigma$  between them, along the  $x$  direction, is not zero [see Fig. 1(a)], the downstream one catches a part  $Q_\Phi$  of the volume lost by the upstream one, proportional to the ratio  $s$  between the overlap length  $\sigma$  and the upstream dune size  $w'$ :

$$s = \frac{\sigma}{w'}, \quad (3)$$

$$Q_\Phi = s\Phi. \quad (4)$$

This defines an effective remote interaction of range  $d_0$  between dunes. Dunes exchange continuous amounts of volume.

If there are several dunes upstream within the distance  $d_0$ , the total caught volume is a sum over all these neighbors, taking into account the screening effect of a dune before one another.

As the speed of a dune is inversely proportional to its size, small dunes travel faster than big ones, and therefore dunes can collide. A collision occurs when two dunes overlap along the  $x$  direction, and the center of mass of the upstream dune passes the center of mass of the downstream one in the  $y$  direction. We emphasize that dunes of our model are cubic, so their physical extents allow collisions on a continuous space. However time is discretized. Therefore we need to test whether a collision happens during a time step  $\Delta t$  or not. A collision is defined by the fact that the ordinates of two dunes will be equal within  $\Delta t$ . We fix the time step at  $\Delta t = 1$ . The mobility  $\alpha$  [see Eq. (1)] is used to tune the rate of the dynamics. In the following, the system is studied for a given maximum time:  $10^5 \Delta t$ .

We impose that the total volume engaged during a collision is conserved, and that a collision only modifies the volume repartition between dunes. Collision phenomenology is entirely determined by its local geometry. The overlap between the two dunes defines sections of the downstream one. These sections are considered separately for the resolution of the collision. The ordinates of the dunes after collision are set to the ordinate of the previous downstream dune. Their abscissas are calculated as the barycenters of the sections they are made of, which can lead to some effective lateral diffusion. We define four types of binary collision [see Fig. 1(b)], depending on the value of the parameters  $s$  [defined in Eq. (3)] and  $r$  defined with the width  $w$  of downstream dune as follows:

$$r = \frac{\sigma}{w}. \quad (5)$$

When the overlap is complete ( $s = 1$ ), we compare  $r$  to a limit value  $\epsilon_t$ . If  $r < \epsilon_t$ , the two dunes merge; if  $r > \epsilon_t$ , the collision rearranges the total volume between the two dunes. The overlapped section of the downstream dune becomes independent, the remaining sections are merged with the upstream dune. If the overlap is not complete ( $s < 1$ ), we compare  $r$  to another limit value  $\epsilon_p$ . If  $r < \epsilon_p$ , the collision splits the downstream dune into two dunes; if  $r > \epsilon_p$  the volume is rearranged between the two dunes as the ( $s = 1, r > \epsilon_t$ ) case. The quantitative effect on the volumes is summarized in Eq. (6), where braces mark individual dunes and brackets mark dune conformations:

$$\left[ \begin{array}{c} \{w^3\} \\ \{w^3\} \end{array} \right] \rightarrow \begin{cases} [\{w^3 + w^3\}] & s = 1, r < \epsilon_t \\ \left[ \begin{array}{c} \{\sigma w^2\} \\ \{w^2(w - \sigma)\} \\ \{w^3\} \end{array} \right] & s < 1, r < \epsilon_p \\ \left[ \begin{array}{c} \{\sigma w^2\} \\ \{w^2(w - \sigma) + w^3\} \end{array} \right] & \begin{array}{l} s = 1, r > \epsilon_t \\ s < 1, r > \epsilon_p \end{array} \end{cases} \quad (6)$$

Depending on the volume ratio and on the relative distance along the  $x$  direction, the interactions may smooth out the volume difference, or increase it. They may shift the dunes away, or align them toward the same axis [14].

Eight parameters control the phenomenology of the model (see Table 1): three length scales, three time scales, and two dimensionless parameters. Thus, according to Buckingham [20], we can build four dimensionless,

TABLE I. Parameters of the model: symbols, physical dimensions, significance, and reference values.

$w_m$	$L$	minimum size	0.01
$w_0$	$L$	injection size	0.1
$d_0$	$L$	limit interaction distance	1
$\Phi$	$L^3 T^{-1}$	volume loss rate	
$\lambda$	$L^{-2} T^{-1}$	injection rate	
$\alpha$	$L^2 T^{-1}$	dunes mobility	0.001
$\varepsilon_r$	$\emptyset$	limit value for $r$ when $s = 1$	0.5
$\varepsilon_p$	$\emptyset$	limit value for $r$ when $s < 1$	0.5

independent control parameters. We first define two aspect ratios:

$$\delta = \frac{w_m}{w_0}, \quad (7)$$

$$\Delta = \frac{w_0}{d_0}. \quad (8)$$

We now explicitly denote the three time scales of the system. According to Eq. (2), the lifetime  $\tau_d$  of a single dune is

$$\tau_d = \frac{w_0^3 - w_m^3}{\Phi}. \quad (9)$$

The typical time  $\tau_n$  between two dune nucleations on a typical surface  $d_0^2$  is

$$\tau_n = \frac{1}{\lambda d_0^2}. \quad (10)$$

The typical collision time  $\tau_c$  is defined as the time for the quickest dune to reach the slowest one within the interaction range  $d_0$ , without considering any other phenomenology. If there is no exchange of volume, the slowest dune is  $w_0$  wide. Therefore,  $\tau_c$  is

$$\tau_c = \frac{d_0}{\alpha} \left( \frac{1}{w_m} - \frac{1}{w_0} \right)^{-1}. \quad (11)$$

Then we can build two control parameters that compare these three times:

$$\xi = \frac{\tau_d}{\tau_n} = \frac{w_0^3 - w_m^3}{\Phi} \lambda d_0^2, \quad (12)$$

$$\eta = \frac{\tau_d}{\tau_c} = \frac{w_0^3 - w_m^3}{\Phi} \frac{\alpha}{d_0} \left( \frac{1}{w_m} - \frac{1}{w_0} \right). \quad (13)$$

The first one compares the relative importance of injection and dissipation in the system. For low  $\xi$ , the volume loss predominates; for high  $\xi$ , the injection is the main drive of the system. The second one compares isolated and collisional dynamics. For low  $\eta$ , the dunes' lifetime is low compared to the typical collision time, therefore dunes hardly interact. For high  $\eta$ , dunes experience lots of collisions before disappearing from the field.

Dunes are made of a collection of sand grains under the drive of the wind. And so their kinematics is really nontrivial [see Eq. (1)]. There is no way to consider these objects as isolated systems under classic conservation laws [14]. Even during collisions where the volume is locally conserved [Eqs. (6)], the effective kinetic energy and momentum are

neither conserved. Because of the minimal size  $w_m$ , the dunes' injection  $\lambda$ , and the merging and fragmentation collision, the number of dunes is not conserved either. Neither is the total volume, as the injection rate  $\lambda$  is constant and not tuned to compensate the loss due to  $\Phi$  and the effect of the minimum size  $w_m$ . This system thus follows no conservation law at the scale of the field. Therefore, no prediction of its large scale dynamics or phase diagram can be made on the basis of conservation law arguments, as often done in statistical physics. In this study, we focus on the numerical exploration of its  $(\xi, \eta)$  phase diagram. All the other parameters are kept constant (see Table I). The length scale is thus defined by  $d_0$ , and the time scale by  $\tau_c$ , through  $\alpha$ . We tune  $\xi$  and  $\eta$  by changing the loss rate  $\Phi$  and the injection rate  $\lambda$ .

### III. ANALYSIS OF SYMMETRIES

One can first ask if there are some limits where the dynamics falls onto a well-known class of universality. When the dissipation is set to zero ( $\Phi = 0$ ), no more remote interaction occurs. The only events are the binary collisions, the nucleation, and the disparition of dunes, named  $A$  in the following. Annihilation happens because collisions can split dunes' volume in a continuous manner, so the resulting volume can be less than the minimal volume  $w_m$ . The dynamics of Eq. (6) can be summarized as



The first three rules [(14)–(16)] embed this model in the pair-contact-process class. However, the nucleation process [Eq. (17)] makes the absorbing phase fluctuate around a stationary state. In the Schlögel model [4,8], such a noise is known to smooth out the transition. We would like to understand how the nucleation acts on our peculiar model.

One can also consider a *quasiconservative* limit where the nucleation is set to zero [ $\lambda = 0$  in our dune model or  $\gamma = 0$  in Eq. (17)]. We call it quasiconservative because we suppress the source of sand, but the persistence of dune annihilation still leads to a global decrease of the total volume of sand. In that version, our model has a true absorbing phase and is very close to the pair contact process with diffusion (PCPD). The PCPD model has two states [6,21–23]; one is an absorbing phase where at most one particle diffuses. The second one is made of patches of persistent activity. If the dynamics is figured on a spatiotemporal scheme, those patches appear as percolated clusters along the time direction. Since our dunes move in a ballistic way along the  $y$  direction, one can wonder whether dune aggregates percolate in this direction.

Another way to analyze the rules of our model is to see each dune as a sand pile [see Figs. 2(a) and 2(c)]. Without dissipation, a single pile is stable and can be destabilized by another pile in its neighborhood. This results in a complex reorganization of sand. This is very similar to the

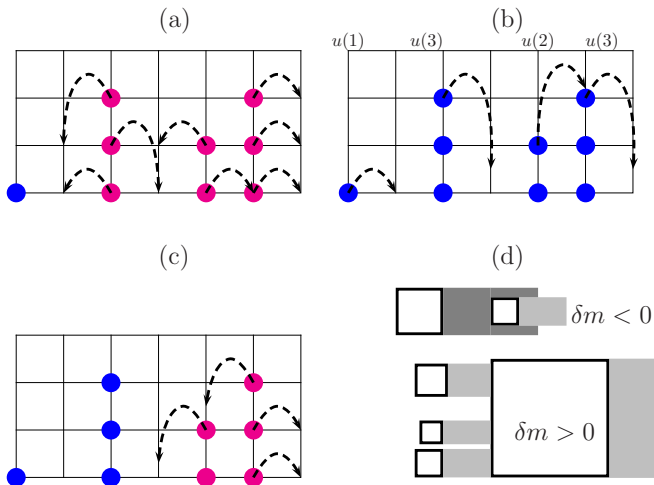


FIG. 2. Definition of sand pile models. (a) BTW-Manna model: a pile of more than one particle is unstable. Then the grains are displaced (randomly) on neighboring sites. (b) Zero range process (ZRP): each grain moves at a rate  $u$  which depends on the occupancy. A variant, the misanthrope model, takes into account the occupancy of the departure and arrival sites. (c) Variant of BTW model where a site is activated by a neighbor. (d) Two configurations of remote sand exchange in our dune model. The dunes are moving from left to right. The shaded spaces figure out the sand which is collected by the wind.

Bak-Tang-Wiesenfeld (BTW) model [24], where piles of grains are unstable above a threshold, but with a condition on the neighborhood (see for instance [25]).

Such a comparison should come with many warnings. In particular, we should discuss whether we are within the framework of self-organized criticality (SOC) [24] as it has been considered for BTW model. It has been shown that SOC and APT are intrinsically linked [26,27]. In SOC, dissipation and driving are equal in magnitude, such that the global density is constant, but their rates are decoupled. The APT counterpart studies a model at a given density and its critical point corresponds to the fixed point of the SOC model. This said, the way the sand is dispatched in our model is deterministic. Deterministic or random input [28] is known to change the stationary properties in a nontrivial way in sand pile models [29,30].

Although all of those points could act on the detailed dynamics, we skip this discussion to concentrate on general aspects. The sand pile model is known to exhibit aggregates which go through the system in avalanches or in multifractal waves, and its transition has common features with critical phenomena. Therefore we expect that our model exhibits a transition to a phase where large aggregates propagate along the wind direction.

These considerations emphasize the role of sand exchange in contrast with reaction process. We can wonder if there is another limit in which reactions are no more the main process and are replaced as the key ingredient by the remote exchange of sand [see Eq. (2) and Fig. 1(a)]. An obvious condition is to set the loss of volume  $\Phi$  to a high level. This sand is lost forever if there are no neighboring dunes, so the global density has also to be sufficiently high to allow interactions. We will show that these conditions are fulfilled at  $\xi \gg 1$  and  $\eta \leq 1$ . In this last

part of the phase diagram, the misanthrope model [31] can be a minimal model to understand our dynamics. In this model, a variant of the zero-range process [see Fig. 2(b)], an element of mass goes from a site  $i$  to the following one (in  $d = 1$ ) with a rate  $u(m_i, m_{i+1})$  which depends on the occupancy of both sites [12,32,33]. Depending on the rate of exchange, the spatial distribution of mass in the system may exhibit a transition. In that case, a small global density will remain homogeneously distributed. But, above a critical density, the excess of mass condenses on a site. The condensate can move, and then the dynamics of mass collection is explosive [32].

Although BTW-like models study unstable dynamics where sudden rearrangements occur and spread like avalanches, the question in MTM is rather to know what type of distribution is reached if sites retain a part of the distributed mass. Indeed it is the main difference. Other ingredients have been changed to test many variants of the models. For instance, both models can be found with a bias toward a direction [34,35], or with nucleation and sinks of matter [12,26,27]. The mass can be discretized, or can be a continuous variable [33,36]. Last, we have pictured these models on one-dimensional space, but they also exist in any dimension. On that peculiar point, even if the motions of barchans occur along the  $y$  direction, the interactions have true two-dimensional aspects as it is depicted in Figs. 1(b) and 2(d).

#### IV. OUT-OF-EQUILIBRIUM STATIONARY STATES

We first focus on the low  $\xi$ , low  $\eta$  region. In this limit, volume loss dominates both the dune injection and the collision dynamics. As shown in [13], the system always reaches a stationary, fluctuating, out-of-equilibrium state in which dunes almost do not interact. The dynamical properties remain normal, in the sense that macroscopic quantities such as fluctuations of the number of dunes are Gaussian [14].

We then decrease the loss rate  $\Phi$ , which means that we travel along the diagonal of the  $(\xi, \eta)$  diagram, to the high  $\xi$ , high  $\eta$  limit. As  $\Phi$  decreases, the density in the field increases and interactions appear. Thus, the phenomenology changes, and clusters of dunes appear in the field. They are created by the destabilization of local high densities through avalanches of collisions. We measured that the fragmenting collisions become dominant in these structures and this generates lots of small dunes, which can then catch up on other dunes. The dynamics of dune birth is no longer Gaussian and this fact supports the idea of avalanche [14].

Inside a cluster, the density is high enough to prevent volume loss: any volume lost by a single dune is caught by the downstream ones. Definitive loss of volume happens mainly at the downstream front of the cluster. Therefore, borders of these structures are very well defined, as any dune put aside by a collision loses volume and quickly vanishes.

Clusters are also responsible for a size selection in the field. As they are very dense, dunes inside go through lots of collisions, whose accumulation leads to the emergence of a new typical size  $\bar{w}$ . Whereas these dunes are small and would disappear quickly in a diluted field, the effective conservation of volume in the clusters stabilizes them. This selection is directly due to the effective dynamics in the clusters and does not happen in the rest of the field. It generates an anticorrelation

between the local density of dunes and the local mean width of dunes [13].

The crossover between dilute and dense dynamics is smooth, and presents no sign that would mark the presence of a phase transition. Quantities of the system evolve without any discontinuity and their fluctuations do not diverge. Neither does the spatial correlation along the  $y$  direction [14]. This crossover is merely a simple, smooth change of dynamics, due to the progressive densification of the system. This can be seen as counterintuitive in the light of the analysis of symmetries (Sec. III). One explanation is that the lifetime of the aggregate is never long enough to allow a clear breaking of symmetry. To stabilize them, one can make the dynamics more conservative in lowering  $\Phi$  and  $\lambda$ . Another possibility is, at a given dissipation  $\Phi$ , to increase the volume injection  $\lambda$ . That is the subject of the next two sections.

## V. PERCOLATION

In the out-of-equilibrium stationary states, a very high activity emerges within the aggregates, although dunes barely interact in the dilute regime. All these states are made of fluctuating populations of objects as far as numbers and volumes of the objects are concerned. However, the dilute regime has some features of an absorbing phase and its fluctuations are given by the nucleation  $\lambda$  and the loss of sand  $\Phi$ . Suppose now that we suppress those two stochastic processes, then the dilute regime will become a true absorbing phase: without direct collision there is no way to produce or destroy dunes.

In the presence of collisions however (see Fig. 1), the number of dunes may fluctuate whereas the total volume is kept constant. So one can wonder whether it is possible to get enough collisions to produce an active phase and a phase transition to this new state. In the following, we address this question first in a quasiconservative system where  $(\Phi, \lambda) = (0, 0)$ . Then we increase the level of fluctuations of the volume  $(\Phi, \lambda) \neq (0, 0)$  to investigate the robustness and the properties of the new phase.

### A. Quasiconservative system

Increasing  $\eta$  as  $\xi$  is kept constant is equivalent to decreasing both the loss rate  $\Phi$  and the injection rate  $\lambda$  in the same manner, and thus lowering the nonconservative aspect of the system. We can even turn off the injection and dissipation. In that case,  $\xi$  is not defined anymore, and  $\eta$  is infinite. Notice that the existence of a minimal size  $w_m$  maintains a sink of matter.

When  $\eta$  is sufficiently high, the behavior changes: the system becomes sensitive to the initial conditions and exhibits a percolation threshold when the initial density increases [Fig. 3(b)]. This transition is rather unusual, as it is a percolation of polydisperse, moving, interacting dunes on a continuous space. Some systems with equivalent features have been previously studied: continuous isotropic percolation of identical disks [37], or squares and other anisotropic objects [38–40]. Some other models describe systems with an infinite number of degrees of freedom [41].

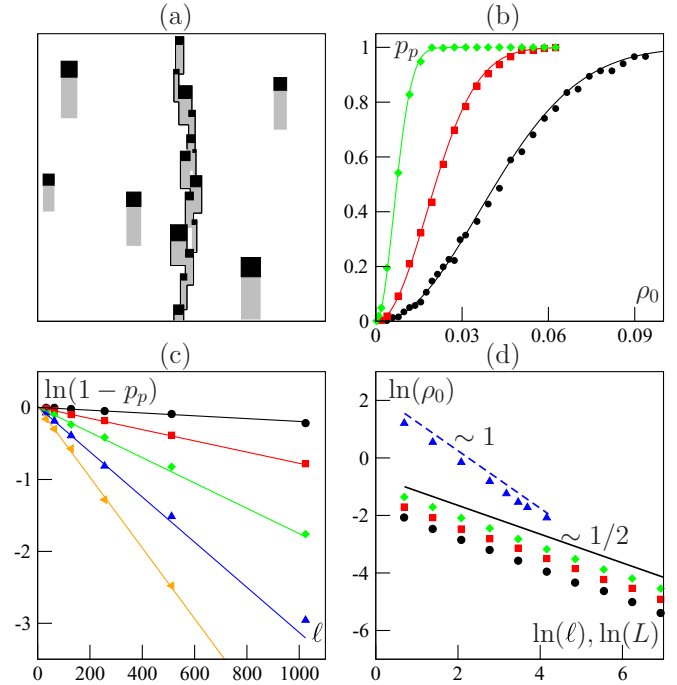


FIG. 3. Percolation. (a) Diagram of a percolation event on the field. Black areas are the proper surfaces of the dunes, gray areas are their interaction surfaces. The surface surrounded in black shows the cluster of dunes that percolates through the periodic boundaries. (b) Probability  $p_p$  for the system to percolate as a function of the initial density  $\rho_0$ , with  $\Phi = 0$  and  $\lambda = 0$ , at a fixed length  $L = 16$ , for different widths of the field:  $\ell = 32$  (●), 128 (■), 1024 (◆). The continuous lines are given by Eq. (20) without any fitting parameter. (c)  $\ln(1 - p_p)$  vs  $\ell$  for a fixed system length  $L = 16$  and different initial densities [ $\rho_0 \simeq 0.0039$  (●), 0.0078 (■), 0.0117 (◆), 0.0156 (▲), 0.0195 (◀)]. The continuous lines are given by Eq. (21) without any fitting parameter. (d) Finite-size effects on the percolation transition. We plot the initial density  $\rho_0$  needed to get a certain probability  $p_p^0$  for the system to percolate: when  $\ell$  varies and  $p_p^0 = 0.25$  (●), 0.5 (■), 0.75 (◆),  $L = 16$ ; when  $L$  varies and  $p_p^0 = 0.978$  and  $\ell = 2$  (▲). The black continuous line shows a power law of exponent  $-1/2$ , the dashed (blue) line shows an exponent of 1.

### 1. Description

Each dune of size  $w$  defines an interaction area of length  $d_0$  and width  $w$  in front of itself. The surface of a dune is defined as the reunion of the proper surface  $w^2$  of the dune and its interaction surface  $wd_0$ . We call percolation the onset of a path that connects the upper and the lower border of the field through overlaps of dunes surfaces, and whose extremities connect themselves through the periodic boundaries [Fig. 3(a)].

We compute the probability of percolation in counting the number of percolated events for a given computation time. This probability  $p_p$  evolves as the initial density  $\rho_0$  is changed [see Fig. 3(b)]. We thus define numerically a threshold  $\rho$  when the probability reaches a given value  $p_p^0$ .

Studying this probability allows us to check the existence of percolated clusters with a low numerical effort. It is however not the classical order parameter. To investigate the properties

of the phase transition, one has to study the probability for a dune to be inside an infinite aggregate.

Finite-size effects show that when the width  $\ell$  of the field increases, the threshold tends to zero with a  $\ell^{-1/2}$  law [Figs. 3(b) and 3(d)]. If the length is increased, the threshold vanishes as  $L^{-1}$  [Fig. 3(d)]. We emphasize that three very different values of  $p_p^0$  have been used to produce Fig. 3(d). So the whole curve is going to be steeper and steeper as the width is increased. Therefore, we could deduce that this percolation could appear at a zero density for an infinite system.

This result is quite astonishing in the light of former studies of percolation on a continuous space [37], and for different shapes of objects [38–40]. Therefore, something in this analogy must be misleading. Indeed, the process which leads to a percolation event is the fruit of dynamical interactions: there is no percolation without collisions.

In the limit of a quasiconservative system, we propose to assume that a percolation event is the result of the interaction of two dunes, which collide with each other and their daughters many times because of the periodic boundary conditions, generating many new dunes in their column and thus forming the percolating cluster. Following this hypothesis, the system is then entirely determined by its initial configuration, as there is no nucleation. The probability for the system to percolate is therefore simply the probability to find at least two dunes in the same column.

## 2. Analytic arguments

Considering that an aggregate is the consequence of an avalanche of fragmenting collisions, let us consider how many interacting dunes are needed to create a percolation event. Initially, the system is fed with a homogeneous distribution of dunes with a mean size  $w_0$ . For the system to percolate, one must have at least two dunes of mean size  $w_0$  in the same column, colliding and then generating through multiple collisions a minimal percolation structure, i.e., a column of length  $L$ , of dunes of minimal size  $w_m$ , each separated from the next downstream one by a length  $d_0$ . So, to ensure that the two initial dunes gather enough volume to generate the minimal percolation structure, one has the mass balance:

$$\frac{L}{d_0} w_m^3 \leq 2w_0^3, \quad (18)$$

for a binary collision. Reversing this argument, we define here the maximum size  $L_2$  for a binary collision to create a percolation event. For a longer system, one has to consider collisions with a greater number of dunes. For a collision with a number  $\mathcal{N}$  of similar dunes, the percolating cluster can reach a length of

$$L_{\mathcal{N}} = \mathcal{N} d_0 \left( \frac{w_0}{w_m} \right)^3. \quad (19)$$

There is no other role of the length in the quasiconservative system. Since dunes do not lose any sand when they are isolated, the longitudinal distance delays the appearance of the percolation, but does not prevent it in any other manner.

The width of the system might change the probability of percolation since the type of collision changes according to the relative lateral position of dunes. For two similar dunes of

width  $w_0$ , their relative distance along the  $x$  direction has to be less than  $\varepsilon_p w_0$  [see Fig. 1 and Eqs. (5) and (6)]. But collisions are symmetric along the axis of motion. Therefore, the cross section of this binary collision is  $d = 2\varepsilon_p w_0$ . Following our hypothesis, the percolation probability  $p_p$  might be the probability to find at least two dunes of size  $w_0$  in a column of width  $d$ . We compute the complementary probability, namely the probability to find no more than one dune in a column  $p(n \leq 1)$ . We also assume that there are only few dunes, so that the number of dunes  $N = \rho_0 L \ell$  is such as  $N \leq \ell/d$ . We define  $k = \ell/d$ , the number of cross-section wide columns within the field, then we find

$$p(n \leq 1) = \frac{k(k-1) \cdots (k-N+1)}{k^N} = \frac{k!}{k^N (k-N)!}. \quad (20)$$

In Fig. 3(b), we show the probabilities of percolation  $p_p$  obtained by changing  $N$  while keeping all the other parameters constant, for different widths  $\ell$  of the system, and compare the previous analytical result to these measures. We show that this simple analytic argument models very well the data without the need of any fitting parameter.

## 3. Finite-size effects

We already have shown that the probability of percolation changes from a system to another with different sizes [Fig. 3(b)–3(d)]. Since the percolation happens in the axis of motion, and while there is some lateral diffusion, length and width act differently on the value of  $p_p$ . So we look at the finite-size effects in decorrelating width and length.

Keeping the length constant, we define  $\kappa = \rho L d$ . Then, remembering that  $k = \ell/d$ , we rewrite the denominator of Eq. (20),  $k - N = k(1 - \kappa)$  which can be taken arbitrarily large for any  $\kappa < 1$ . So we use Stirling's approximation in Eq. (20) and we find the following scaling when  $k \rightarrow \infty$ :

$$\ln[p(n \leq 1)] \sim -[(1 - \kappa) \ln(1 - \kappa) + \kappa]k - \frac{1}{2} \ln(1 - \kappa). \quad (21)$$

We indeed observe that the percolation probability,  $p_p = 1 - p(n \leq 1)$ , tends to 1 exponentially as the width is increased, see Fig. 3(c), following the exact scaling of Eq. (21).

The constraint  $\kappa < 1$  is reminiscent of the fact that a greater number of dunes than the number of columns obviously leads to a percolated system. So, if we keep  $\ell$  constant and increase the length  $L$  at a given density, the probability of percolation increases to 1 where we expect  $\kappa \sim 1$ :

$$p_p \sim 1 \Rightarrow \rho_0 \propto \frac{1}{L}. \quad (22)$$

We observe such a scaling on data, Fig. 3(d), for relatively small system sizes ( $L \leq 64$ ). Simulating larger systems is just a matter of computation time. Let us also point out the fact that our numerical systems were never long enough to test the mass balance of a percolating cluster [Eq. (19)]. But one can have an idea of the effect of  $L$  using our probability model: when  $L \leq L_2$ , only binary collisions occur. If  $L \in [L_{\mathcal{N}-1}; L_{\mathcal{N}}]$ , one has to consider collisions involving  $\mathcal{N}$  dunes.

In other words, we have to study the probability to find at least  $\mathcal{N}$  dunes in one column. We assume that the cross section remains  $2\varepsilon_p w_0$ . To argue for this point, let us decompose the

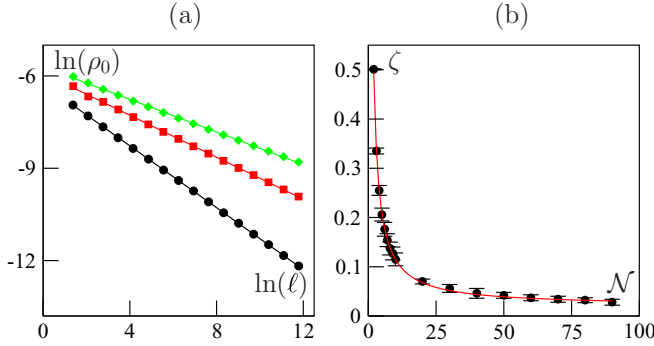


FIG. 4. Size effects in the probabilistic model. (a) Initial density  $\rho_0$  which leads to a probability of percolation of  $p_p = 1/2$  vs  $\ell$  and for different  $\mathcal{N} = 2$  (●), 3 (■), and 4 (◆). The plain lines are fitting curves which correspond respectively to an exponent  $\zeta$  of 0.5, 0.35, and 0.28 (in  $\ln$ - $\ln$  scale). (b) Exponent  $\zeta$  for the number  $\mathcal{N}$  of colliding dunes. The plain line is the best algebraic fit:  $\zeta \simeq 0.020 + 0.95/\mathcal{N}$ .

interaction of three dunes into two collisions. In the first one, if positions of dunes are homogeneous, the mean lateral position is  $\varepsilon_p w_0/2$ , which leads to a new dune with a volume  $\varepsilon_p w_0^3/2$ , or a width  $w_1 = w_0(\varepsilon_p/2)^{1/3}$  [see Eq. (6)]. The latter bumps into a dune of mean width  $w_0$ , for which the maximum cross section is  $\varepsilon_p w_0$ . We notice also that  $w_1 \geq \varepsilon_p w_0$  as soon as  $\varepsilon_p \leq \sqrt{2}/2$ . In our simulations  $\varepsilon_p = 0.5$ , therefore the cross section is the maximal cross section. Considering the symmetry along the axis of motion, we conclude that the discretization of the space in  $2\varepsilon_p w_0$ -wide columns is still valid.

We computed the probability  $p(n \geq \mathcal{N})$  to find at least one column of width  $d$  with at least  $\mathcal{N}$  over a total number  $N$  of dunes at a given width  $\ell$ . For small lengths, we observe in Fig. 4 that the percolation threshold, defined as  $p(n \geq \mathcal{N}) = 1/2$ , vanishes as  $\ell^{-\zeta}$ . But the exponent decreases with the number of dunes  $\mathcal{N}$ . The data are consistent with a nonvanishing asymptotic value for  $\zeta$ , which would mean that the transition occurs at any density for any width and length in this mean-field model.

### B. Percolation with fluctuations

In the quasiconservative system, the control parameter of the percolation is the initial density of dunes  $\rho_0$  in the field. The randomness is due to the initial conditions, that then determine entirely the evolution of the system. On the contrary, the stationary phase at low values of  $(\xi, \eta)$  is stochastic, independent of the initial condition [14] and the stationary density is set by the dynamics to  $\rho = \xi/d_0^2$ . So, we now question the existence of a percolation phase in a stochastic nonconservative system, even though there are only few events of nucleation per time step.

Indeed, the system still percolates. We scanned the  $(\xi, \eta)$  diagram and measured the probability of percolation  $p_p$  at a given initial density  $\rho_0$ ; see Fig. 5(a). We observe a zone where the system never percolates, and a region where percolation becomes likely. The probability to percolate seems to vary linearly between both regions and become steeper as the system size is increased. Finite-size effects thus confirm the existence of two regions: with or without percolated cluster even in the presence of dissipation and nucleation [Fig. 5(b)].

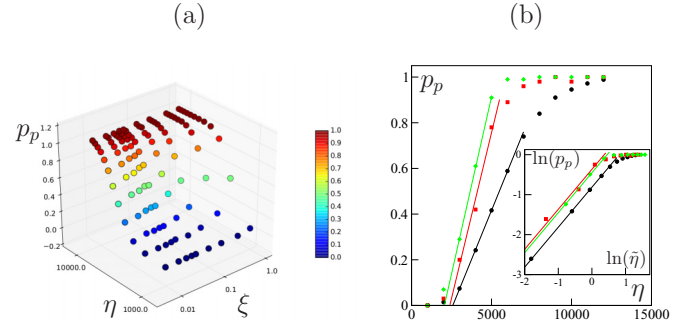


FIG. 5. Percolation in nonconservative systems. (a) Phase diagram for different sets of parameters  $(\eta, \xi)$  at a fixed system width  $\ell = 32$  in log-log scale. The color map indicates the magnitude of percolation probability: the probability decreases with increasing  $\eta$ . (b) Transitions at  $\xi = 0.01$  for varying  $\eta$  and for different system widths  $\ell = 32$  (●), 64 (■), 128 (◆). The continuous lines are linear fits of the data. In the inset, the same data in  $\ln$ - $\ln$  curve, with  $\tilde{\eta} = 1 - \eta/\eta_c$ . Other parameters of simulation:  $\rho = 1/8$  and  $L = 32$ .

At rather small system sizes, the behavior of the system turns out to depend on the initial density  $\rho_0$ . As the density increases, the percolation is more and more likely (data not shown). But the transition line in the  $(\xi, \eta)$  diagram is not shifted by the variation of the initial density. As we have shown that percolation appears in a quasiconservative system even at very low density for a very large system, we may think that this dependency is a finite-size effect. We observe that the percolation probability also increases when the system size is increased. The number of nucleations increases with the system size; it makes the system more stochastic, but it also feeds the system with an amount of sand and makes the percolation likely to appear. Hence, it allows the system to lose the memory of its initial conditions.

### C. Percolation dynamics

A percolation event is not a stationary pattern, even for a quasiconservative system. Fragmenting collisions split dunes, whatever their sizes, into smaller objects. They can thus become smaller than the smallest possible dune, and disappear. That is why an avalanche of collisions that created a percolated cluster erodes it after a while. For any finite  $\eta$ , volume loss occurs. However we expect it has little effect on a percolated aggregate, since a cluster is a zone where sand is almost a conserved quantity. The process which will dominate the dynamics of percolation will thus be the nucleation.

Indeed, for high values of  $\eta$ , the system easily percolates for any value of  $\xi$ . However, the temporal evolution of the system differs a lot along the  $\xi$  range. Percolation usually occurs the first time during the transient regime. Then, the system can rebuild a percolating situation through nucleation, and other events can occur. This rebuilding takes a certain time, related to the nucleation rate. Furthermore, not all clusters percolate, which reduces again the probability for the system to present such an event. In Fig. 6(a) we clearly see bursts of the number of dunes, each signing the apparition of a cluster in the field, but only one succession of percolation events. For low  $\xi$ , the time between two series of percolation events is thus very

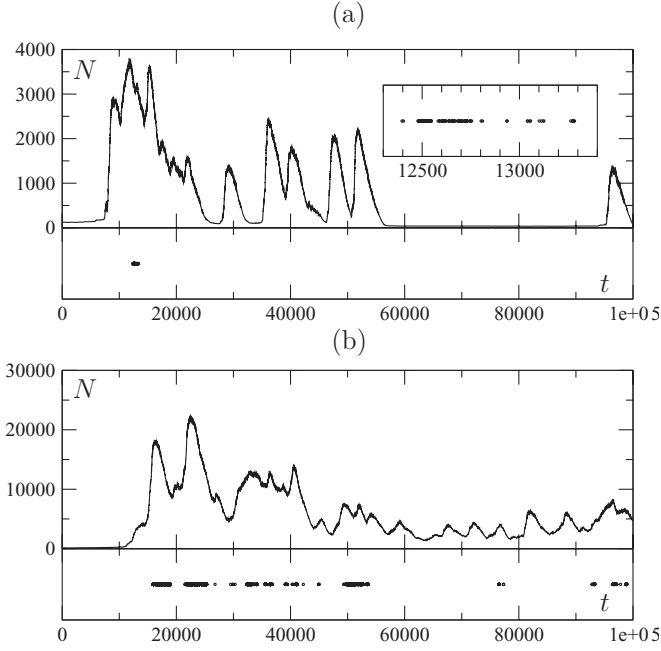


FIG. 6. Modes of percolation. Evolution of the number of dunes in the field (top of each subfigure) and events of percolation (bottom) at a given  $\eta = 10^4$  and for two different  $\xi$ :  $\xi = 0.01$  in (a) and  $\xi = 1$  in (b). The inset shows a zoom of the only succession of percolation events that occurs in (a). Other parameters of simulation:  $\rho = 1/8$  and  $L = \ell = 32$ .

large. For high  $\xi$  this time tends to become rather small as the nucleation is more important and rapidly refills the field. Indeed, in Fig. 6(b) we have percolation series along the whole simulation.

There are thus two asymptotic modes for the percolable phase, which are closely related to the two modes of the stationary phase: a dilute mode where percolation events are separated by very long times, and a dense mode where percolation events occur much more often. As for the stationary phase, a smooth crossover connects these two modes. Moreover, in the  $(\xi, \eta)$  space the two crossovers have the same structure, connected above the phase transition line. This points out that there might actually be only one dynamical crossover, coming on top of the phase diagram (Fig. 8).

## VI. GIANT DUNES INSTABILITY

We now focus on the opposite limit, where  $\eta$  is kept constant at a low value and  $\xi$  increases. In this limit, the volume loss is kept at a high value by  $\eta$ , and the nucleation rate increases with  $\xi$ . This is therefore a limit of high forcing and dissipation.

When we increase the injection rate, the system is first homogeneous and stationary. Then a critical  $\xi$  appears beyond which the steady state becomes unstable. After some time, the sizes of several dunes begin to grow and never saturate [Fig. 7(a)]. If the fixed value of  $\eta$  is very low, this instability occurs in a rather diluted field, with few collisions. For higher values of  $\eta$ , a collisional stage occurs before the instability starts [Fig. 7(b)]. As for both previous phases, this defines two modes for the instability.

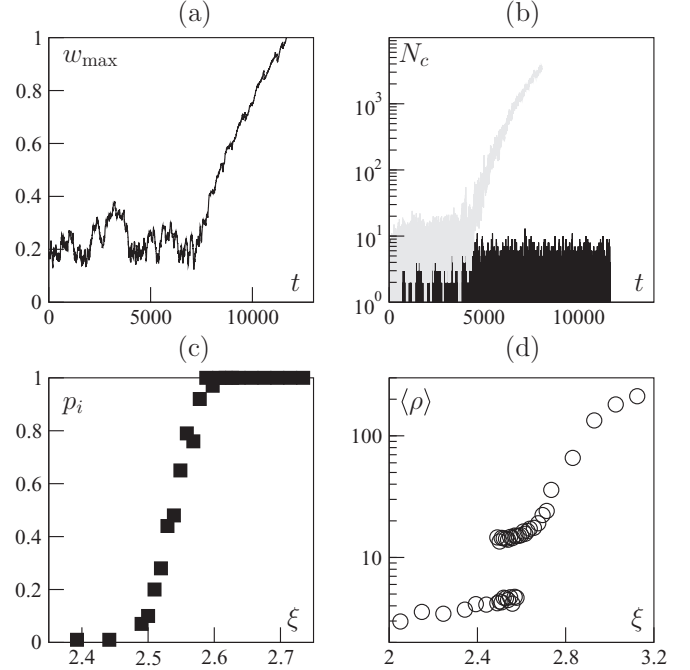


FIG. 7. Giant dunes instability. (a) Size of the biggest dune in the field, as a function of time, for  $\xi = 2.15$  and  $\eta = 0.3$ . (b) Collision rate as a function of time, for  $\xi = 2.15$  and  $\eta = 0.3$  (black) and  $\xi = 2.73$  and  $\eta = 1$  (gray). (c) Probability for the system to be unstable as a function of  $\xi$ , for  $\eta = 1$ . (d) Mean density  $\langle \rho \rangle$  at the end of the simulation as a function of  $\xi$ , for  $\eta = 1$ , calculated on 100 realizations. For other parameters, see caption of Fig. 6.

In the noncollisional mode, the system reaches a metastable state before the instability starts [Fig. 7(a)]. For both modes, there is no precise, critical value for  $\xi$  but a range of values where the probability for the system to develop the instability grows continuously from 0 to 1 [Fig. 7(c)]. Furthermore, the mean values of physical observables—for example the density—measured at the end of the simulation, present two disconnected branches, for the stable and the unstable phase [Fig. 7(d)]. The observation of metastability and hysteresis is an indication of the fact that the instability is subcritical.

The instability can appear in a low collisional system, therefore its origin is probably not the merging type of collision. Indeed, a toy model where a dune of size  $w$  is randomly impacted by dunes of size  $w'$  shows that even for very large  $w$ , no instability involving only collisions can appear. Even though the coalescence could in theory continuously increase the size of a dune, the fragmentation is far more efficient at decreasing this size (Fig. 1).

The mechanism of the giant dunes' instability rather involves the remote interaction through volume exchange. The field at low  $\eta$  and high  $\xi$  contains a high number of dunes, whose lifetimes are very small due to the high volume loss. There are thus lots and very important volume exchanges in the field. Every dune loses a volume  $\Phi$  per unit of time, but also gathers sand lost by any other upstream dunes. The balance of sand strongly depends on the dune width [see Fig. 2(d)]. For instance, let a dune of size  $w$  be followed by several dunes of size  $w_m$  (which will disappear next time step). The maximum



sand balance will be when dunes cover its whole size:

$$\frac{dV}{dt} = -\Phi + \Phi \frac{w}{w_m}. \quad (23)$$

The small dunes will feed the large one and disappear without having the time to collide with it. So any local fluctuation of a dune's density behind a larger dune will make the latter grow, thus increase its lifetime, and its ability to collect more sand. If the injection rate is high enough, these collecting events are numerous enough to make the size of some particles diverge, and generate the instability.

The crossover from noncollisional to collisional instability is smooth. As for the percolable phase, it is in fact the same crossover that exists between dilute and dense stationary states.

## VII. CONCLUSION

### A. Summary

We explored in this paper the phase diagram of a nontrivial system. The effective energy and momentum as well as the number of dunes and the total volume of these dunes are not conserved at the scale of the whole system. The model has a peculiar phenomenology, inspired by the geophysical problem of barchan fields. In particular, dunes interact with each other through nontrivial collisions and remote volume exchange. Dunes are injected in the field, while volume loss at each one of them ensures they have a finite lifetime. Two parameters, comparing forcing and dissipation for  $\xi$ , isolated and interacting behavior for  $\eta$ , define the phase diagram.

For standard values of the parameters, the system always reaches a stationary state. Its dynamics range smoothly from noninteracting to interacting as both parameters increase, and are independent of the initial conditions.

When  $\eta$  becomes large, i.e., when the dissipation decreases, the system becomes percolable, meaning that depending on the initial density the system can exhibit a percolation transition. This percolation is unusual, as it occurs on a continuous space with polydisperse, moving, finite lifetime, interacting objects. Indeed, we show that for a system with an infinite width, percolated aggregates are likely to appear for any small value of density. An analytic, mean-field, probabilistic model reproduces well the behavior of the probability to percolate. We extend the study of this model on the effects of the system length, and it gives clues to suppose that percolation is robust also when the length is increased. Similarly to the stationary phase, dynamics range from dilute, where percolation events are sparse in time, to dense, where they occur much more often.

When  $\xi$  becomes large for low  $\eta$ , i.e., when both dissipation and forcing are large, the system becomes unstable. Trapped in local high densities, the sizes of some of the dunes grow without limit. The instability, characterized by a discontinuity in the evolution of the system observables, by a range of coexistence between stable and unstable phase, and by a metastability before the beginning of the instability, is subcritical. As for the previous phases, its dynamics smoothly range from noncollisional, where the collision rate is low before the instability, to collisional, where the instability begins after a large increase of the collision rate.

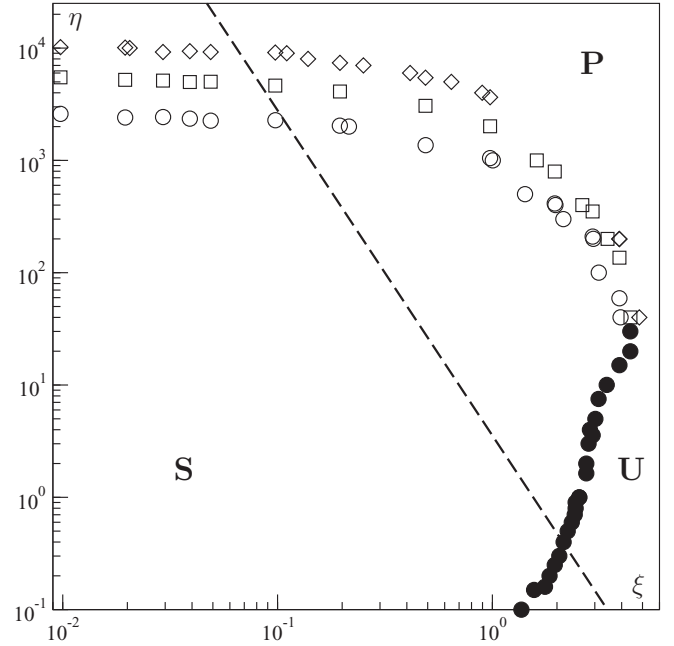


FIG. 8. Phase diagram of the system. **S** is the stationary phase, **P** is the percolable one, **U** is the unstable one. The frontier between **S** and **P** is marked by three isolines for the probability for the system to percolate with  $\rho_0 = 1$ :  $p_p = 0.05$  ( $\circ$ ),  $p_p = 0.5$  ( $\square$ ),  $p_p = 0.95$  ( $\diamond$ ). The frontier between **S** and **U** is marked by the isoline for the probability for the system to be unstable,  $p_i = 0.5$  ( $\bullet$ ). The dashed line marks the smooth crossover from noncollisional to collisional dynamics. Other parameters are the same as in Fig. 6.

A smooth phase transition separates the stationary and the percolable phase, a coexistence range separates the stationary and the unstable phase, whereas the limit between percolable and unstable remains unknown. In the end, the phase diagram of the system seems to consist of the three previous proper phases, plus a dynamical diagram on top of it. Indeed, the smooth range of dynamics from noncollisional to collisional is found on all three phases, and is connected through their limits (Fig. 8). The parameters  $\xi$  and  $\eta$  thus define both the phase of the system, and the dynamics this phase is exhibiting.

### B. Analogies and future work

Changing the relative values of  $\xi$  and  $\eta$  changes the relative weight of the exchange of volume in the remote interaction [Eqs. (2)–(4)] compared to the local collisions [Eq. (6)]. When collisions dominate, we indeed found percolated clusters as in absorbing phase transition models. When eolian transfer of mass is more frequent, mass condensation occurs as in the mass transfer model.

First, both regions are connected by a domain of the phase diagram whose properties deserve to be studied. Next, percolation seems to survive to fluctuations in contrast to classical results on the Schlögel model. However this result is not so much questioned. First fluctuations remain at a low level ( $\xi \leq 1$ ) when percolation is likely. Second, when fluctuations increase in comparison to dissipation, there is a smooth crossover between noncollisional and collisional dynamics and this crossover is not a phase transition. A last

interesting test would be to modify the nucleation process in order to have a true absorbing phase: for instance one can nucleate a new dune close to a previously existing dune.

Obviously, one has to characterize the phase transition of percolation in our model. In Eqs. (14) and (15), rates of reaction depend on  $\eta$  and  $\xi$  but also on thresholds  $\varepsilon_p$  and  $\varepsilon_t$ . Therefore we could expect that the transition of percolation should depend on them. But it is surprising that we do not need  $\varepsilon_t$  in our mean-field approximation.

The last region of the phase diagram is reached when the remote exchange of sand dominates. We then observe a

first order phase transition of condensation. Mass transport models exhibit also a phase with a condensate. Their stationary solutions are usually made of two asymptotic phases: one is a nearly homogeneous density, the second is made of a condensation of the excess mass to the latter homogeneous repartition [31]. In some cases the dynamics of condensation can be explosive [32] and the condensate visits ballistically the system. However, it seems to us that the existence of a metastable state is an unusual feature of this class of model. The explanation of this difference has probably to be found in the nonconservative properties of our model.

- 
- [1] S. Aumaître, S. Fauve, S. McNamara, and P. Poggi, *Eur. Phys. J. B* **19**, 449 (2001).
  - [2] F. Schlögel, *Z. Phys.* **253**, 147 (1972).
  - [3] R. C. Brower, M. A. Furman, and M. Moshe, *Phys. Lett.* **B76**, 213 (1978).
  - [4] P. Grassberger, *Z. Phys. B: Condens. Matter* **47**, 365 (1982).
  - [5] H. Hinrichsen, *Adv. Phys.* **49**, 815 (2000).
  - [6] J. Kockelkoren and H. Chaté, *Phys. Rev. Lett.* **90**, 125701 (2003).
  - [7] M. Rossi, R. Pastor-Satorras, and A. Vespignani, *Phys. Rev. Lett.* **85**, 1803 (2000).
  - [8] S. Prakash and G. Nicolis, *J. Stat. Phys.* **86**, 1289 (1997).
  - [9] T. Vicsek, A. Czirók, E. Ben-Jacob, I. Cohen, and O. Shochet, *Phys. Rev. Lett.* **75**, 1226 (1995).
  - [10] G. Grégoire and H. Chaté, *Phys. Rev. Lett.* **92**, 025702 (2004).
  - [11] A. P. Solon, H. Chaté, and J. Tailleur, *Phys. Rev. Lett.* **114**, 068101 (2015).
  - [12] M. R. Evans and T. Hanney, *J. Phys. A* **38**, R195 (2005).
  - [13] M. Génois, S. Courrech, P. Hersen, and G. Grégoire, *Geophys. Res. Lett.* **40**, 3909 (2013).
  - [14] M. Génois, P. Hersen, S. Courrech du Pont, and G. Grégoire, *Eur. Phys. J. B* **86**, 447 (2013).
  - [15] P. Hersen, *Eur. Phys. J. B* **37**, 507 (2004).
  - [16] P. Hersen and S. Douady, *Geophys. Res. Lett.* **32**, L21403 (2005).
  - [17] R. A. Bagnold, *The Physics of Blown Sand and Desert Dunes* (Chapman and Hall, London, 1941).
  - [18] H. Finkel, *J. Geol.* **67**, 614 (1959).
  - [19] H. Elbelrhiti, B. Andreotti, and P. Claudin, *J. Geophys. Res.* **113**, F02S15 (2008).
  - [20] E. Buckingham, *Phys. Rev.* **4**, 345 (1914).
  - [21] S.-C. Park and H. Park, *Phys. Rev. Lett.* **94**, 065701 (2005).
  - [22] I. Dornic, H. Chaté, and M. A. Muñoz, [arXiv:cond-mat/0505171](https://arxiv.org/abs/cond-mat/0505171).
  - [23] H. Hinrichsen, *Physica A* **361**, 457 (2006).
  - [24] P. Bak, C. Tang, and K. Wiesenfeld, *Phys. Rev. Lett.* **59**, 381 (1987).
  - [25] S. Maslov and Y.-C. Zhang, *Physica A* **223**, 1 (1996).
  - [26] A. Vespignani and S. Zapperi, *Phys. Rev. Lett.* **78**, 4793 (1997).
  - [27] A. Vespignani, R. Dickman, M. A. Muñoz, and S. Zapperi, *Phys. Rev. Lett.* **81**, 5676 (1998).
  - [28] S. S. Manna, *J. Phys. A* **24**, L363 (1991).
  - [29] D. V. Kvitarev, S. Lübeck, P. Grassberger, and V. B. Priezhev, *Phys. Rev. E* **61**, 81 (2000).
  - [30] M. De Menech and A. L. Stella, *Phys. Rev. E* **62**, R4528 (2000).
  - [31] M. R. Evans, *Braz. J. Phys.* **30**, 42 (2000).
  - [32] B. Waclaw and M. R. Evans, *Phys. Rev. Lett.* **108**, 070601 (2012).
  - [33] M. R. Evans, S. N. Majumdar, and R. K. P. Zia, *J. Phys. A* **37**, L275 (2004).
  - [34] T. Hwa and M. Kardar, *Phys. Rev. Lett.* **62**, 1813 (1989).
  - [35] D. Dhar and R. Ramaswamy, *Phys. Rev. Lett.* **63**, 1659 (1989).
  - [36] M. Basu, U. Basu, S. Bondyopadhyay, P. K. Mohanty, and H. Hinrichsen, *Phys. Rev. Lett.* **109**, 015702 (2012).
  - [37] G. Grimmett, *Percolation*, Grundlehren der mathematischen Wissenschaften Vol. 321, 2nd ed. (Springer, Berlin, Heidelberg, 1999).
  - [38] D. R. Baker, G. Paul, S. Sreenivasan, and H. E. Stanley, *Phys. Rev. E* **66**, 046136 (2002).
  - [39] S. Mertens and C. Moore, *Phys. Rev. E* **86**, 061109 (2012).
  - [40] Z. Koza, G. Kondrat, and K. Suszczyński, *J. Stat. Mech.: Theory Exp.* (2014) P11005.
  - [41] L. Corté, P. M. Chaikin, J. P. Gollub, and D. J. Pine, *Nat. Phys.* **4**, 420 (2008).